Heat shock protein family D member 1 mediates lung cancer cell-induced angiogenesis of endothelial cells

KEERAKARN SOMSUAN[1,2], ARTITAYA RONGJUMNONG[2], ATTHAPAN MORCHANG[1,2], PHATEEP HANKITTICHAI[1,2], JATUPORN NGOENKAM[3], ANUPONG MAKEUDOM[4], KRIENGSAK LIRDPRAPAMONGKOL[5], SUTTICHAI KRISANAPRAKORNKIT[4], SUTATIP PONGCHAROEN[6], JISNUSON SVASTI[5] and SIRIPAT ALUKSANASUWAN[1,2]

[1]School of Medicine, Mae Fah Luang University, Chiang Rai 57100, Thailand; [2]Cancer and Immunology Research Unit, Mae Fah Luang University, Chiang Rai 57100, Thailand; [3]Department of Microbiology and Parasitology, Faculty of Medical Science, Naresuan University, Phitsanulok 65000, Thailand; [4]School of Dentistry, Mae Fah Luang University, Chiang Rai 57100, Thailand; [5]Laboratory of Biochemistry, Chulabhorn Research Institute, Bangkok 10210, Thailand; [6]Department of Medicine, Faculty of Medicine, Naresuan University, Phitsanulok 65000, Thailand

Received January 8, 2025; Accepted February 14, 2025

DOI: 10.3892/br.2025.1955

Abstract. Angiogenesis is a crucial process in lung cancer growth and progression. Heat shock protein family D member 1 (HSPD1 or HSP60) plays a significant role in promoting lung cancer development, but its role in angiogenesis remains largely unexplored. The present study aimed to investigate the involvement of HSPD1 in lung cancer cell-induced angiogenesis using indirect co-culture experiments. Secretomes were collected from stable HSPD1-knockdown A549 lung cancer cells [short hairpin (sh)HSPD1-A549 cells] and scramble control cells (shControl-A549 cells) and used to treat human endothelial EA.hy926 cells. Effects of the secretomes on key steps of angiogenesis, including endothelial cell proliferation, migration, invasion, aggregation and tube formation, were assessed using BrdU incorporation, wound healing, Transwell invasion, hanging-drop and Matrigel tube formation assays, respectively. The amount of vascular endothelial growth factor (VEGF) secreted by EA.hy926 cells was determined using ELISA. The correlation of VEGFA expression with HSPD1 expression and overall survival in patients with lung adenocarcinoma was evaluated using bioinformatics analysis. The results revealed that the shControl-A549 secretome markedly stimulated endothelial cell proliferation, migration, invasion, aggregation, tube formation and VEGF secretion, whereas the shHSPD1-A549 secretome had no significant effects on these processes. VEGFA expression was markedly associated with HSPD1 expression and overall survival in patients with lung adenocarcinoma. In conclusion, the findings highlighted the role of HSPD1 in promoting angiogenesis capability of endothelial cells, potentially through VEGF-mediated pathways. Targeting HSPD1 may represent a promising therapeutic strategy to inhibit angiogenesis and improve clinical outcomes in lung cancer patients.

Correspondence to: Dr Siripat Aluksanasuwan, School of Medicine, Mae Fah Luang University, 333 Moo 1, Thasud, Muang, Chiang Rai 57100, Thailand
E-mail: siripat.alu@mfu.ac.th

Key words: lung cancer, heat shock protein family D member 1, angiogenesis, endothelial cells, vascular endothelial growth factor

Introduction

Angiogenesis, the formation of new blood vessels, is a crucial process in cancer progression, including lung cancer (1,2). Tumor cells and stromal cells in the tumor microenvironment (TME) secrete various molecules that stimulate endothelial cell proliferation and migration, promoting the formation of new blood vessels to supply oxygen and nutrients needed for tumor growth and metastasis (3). Increased angiogenesis and elevated levels of angiogenic factors are associated with poor prognosis in lung cancer (4-6). Recently, inhibiting angiogenesis has gained attention as a therapeutic strategy for lung cancer (2). Drugs targeting vascular endothelial growth factor (VEGF) and receptor tyrosine kinase can inhibit tumor growth and spread; however, their efficacy remains limited (2). Therefore, an improved understanding of the mechanisms driving angiogenesis is essential for the development of more effective therapies for lung cancer.

Angiogenesis is tightly regulated by a balance between pro-angiogenic and anti-angiogenic factors (7). Among the pro-angiogenic factors, VEGF serves as a key player in tumor angiogenesis (8). Previously, it was considered that endothelial cells did not produce VEGF, but the accumulation of evidence indicates that the cells can produce small amount of VEGF for vascular homeostasis and VEGF can act as both a paracrine and an autocrine signaling molecule (9). During tumor growth, hypoxia and conditions within the TME stimulate VEGF expression in endothelial cells to initiate angiogenesis (8,10,11). VEGF binds to its receptors, VEGFR1 and VEGFR2, on

endothelial cells to promote endothelial cell proliferation and survival (8,12). Activated endothelial cells subsequently migrate, invade the extracellular matrix and aggregate with neighboring cells, eventually forming tubular structures that develop into a functional vascular network (7,13).

Heat shock protein family D member 1 (HSPD1), also known as HSP60 or chaperonin 60, is a multifunctional protein implicated in various cancers (14). It has been shown to regulate cancer cell apoptosis, proliferation and metastasis, while extracellular HSPD1 functions as an immune modulator involved in tumor immunity (14,15). Studies highlight its significant role in lung cancer development and progression (16-19). Increased HSPD1 expression is associated with poor prognosis in patients with non-small cell lung cancer (16-18). HSPD1 promotes lung cancer growth by regulating mitochondrial functions (17) and plays a role in modulating the TME (18,19). HSPD1 expression is associated with the infiltration of various immune cells (18). A previous study demonstrates that the knockdown of HSPD1 in lung cancer cells alters the composition of secreted proteins and diminishes its effect on the activation of cancer-associated fibroblasts (CAFs) (19). Evidence also suggests that HSPD1 regulates endothelial cell function and angiogenesis (20-23). Recent findings indicate that the long non-coding RNA LINC01503 promotes angiogenesis in colorectal cancer by increasing VEGFA expression through interactions with microRNA (miR)-342-3p and HSPD1 (24). Collectively, these findings suggest that HSPD1 may play a pivotal role in regulating angiogenesis. However, its specific role in lung cancer remains unclear and needs further elucidation.

The present study aimed to investigate the involvement of HSPD1 in lung cancer cell-induced angiogenesis using indirect co-culture experiments. The effects of secretome derived from HSPD1-knockdown lung cancer cells on the angiogenic properties of endothelial cells were investigated, in comparison with secretome from control cells. Angiogenic behaviors, including cell proliferation, migration, invasion, aggregation and tube formation, were evaluated in endothelial cells following secretome treatment. VEGF secretion levels from endothelial cells were measured. Finally, the correlation of VEGFA expression with HSPD1 expression and overall survival in patients with lung adenocarcinoma was analyzed using bioinformatics. The findings of the present study provided new insights into the role of HSPD1 in promoting tumor angiogenesis of lung cancer. Targeting HSPD1 may be a potential therapeutic strategy to inhibit angiogenesis and tumor progression in lung cancer patients.

Materials and methods

Cell culture. Human lung cancer A549 (CCL-185) and human endothelial EA.hy926 (CRL-2922) cell lines were obtained from the American Type Culture Collection (ATCC). Knockdown of HSPD1 in A549 cells was achieved using a shRNA-lentiviral system, as previously described (19). Stable HSPD1-knockdown (shHSPD1-A549) and shControl-A549 cells were maintained in Dulbecco's Modified Eagle's Medium (DMEM; Gibco; Thermo Fisher Scientific, Inc.) supplemented with 10% (v/v) fetal bovine serum (FBS; Gibco; Thermo Fisher Scientific, Inc.) and 1 μg/ml puromycin. EA.hy926 cells were cultured in DMEM supplemented with 10% FBS, 100 IU/ml penicillin G and 100 μg/ml streptomycin. All cells were incubated at 37˚C in a humidified incubator with 5% CO_2.

Establishment of shHSPD1-A549 and shControl-A549 cells. shHSPD1 with the following oligonucleotide sequence: 5'-GCTAAACTTGTTCAAGATGTTTCAAGA GAACATCTTGAACAAGTTTAGCTTTTTT-3' was cloned into the pLKO.1-puro plasmid (a gift from Dr Bob Weinberg, Whitehead Institute for Biomedical Research and Department of Biology, Massachusetts Institute of Technology, MA, USA; Addgene plasmid no. 8453). The scrambled shRNA (shControl) with the oligonucleotide sequence: 5'-CCTAAGGTT AAGTCGCCCTCGCTCGAGCGAGGGCGACTTAACCTT AGG-3' inserted into the pLKO.1-puro plasmid (a gift from Dr David Sabatini, Whitehead Institute for Biomedical Research and Department of Biology, Massachusetts Institute of Technology, MA, USA; Addgene plasmid no. 1864) served as a negative control. Using a third-generation lentivirus system, lentiviral particles were produced by co-transfecting 293T cells (CRL-3216; ATCC) with either pLKO.1-puro-shHSPD1 (6 μg) or pLKO.1-puro-shControl (6 μg), along with packaging plasmids, including pMDLg/pRRE (a gift from Dr Didier Trono, Department of Genetics and Microbiology, Faculty of Medicine, University of Geneva, Switzerland; Addgene plasmid no. 12251), pRSV-Rev (a gift from Dr Didier Trono, Addgene no. 12253), and pCMV-VSV-G (a gift from Dr Bob Weinberg, Addgene plasmid no. 8454) using jetPRIME transfection reagent (Polyplus) for 12 h at 37˚C. At 24 h post-transfection, the viral supernatant was harvested and used to transduce A549 cells at a multiplicity of infection of 10 in the presence of polybrene (4 μg/ml) at 37˚C for 24 h. Stable shHSPD1-A549 and shControl-A549 cells were selected using puromycin (1 μg/ml) for ~1 week. Knockdown efficiency was confirmed by western blot analysis.

Western blot analysis for assessment of knockdown efficacy. Protein was extracted from shHSPD1-A549 and shControl-A549 cells using RIPA buffer (Abcam). Protein concentrations were determined by the Bradford assay (Bio-Rad Laboratories, Inc.). Equal amounts of protein from each sample (20 μg) were separated via 12% SDS-PAGE and transferred onto a nitrocellulose membrane. The membrane was blocked with 5% (w/v) skimmed milk in phosphate-buffered saline (PBS) at room temperature for 1 h. Subsequently, the membrane was incubated overnight at 4˚C with either rabbit monoclonal anti-HSPD1 (1:1,000; cat. no. 12165; Cell Signaling Technology, Inc.) or mouse monoclonal anti-GAPDH (1:5,000; cat. no. ab8245; Abcam). After three washes with PBS containing 0.05% (v/v) Tween 20 (PBS-T), the membrane was incubated with horseradish peroxidase-conjugated secondary anti-rabbit IgG (1:5,000; cat. no. ab6721; Abcam) or anti-mouse IgG (1:5,000; cat. no. ab205719; Abcam) antibodies at room temperature for 1 h. Immunoreactive bands were visualized using Clarity Western ECL Substrate and captured with the ChemiDoc Touch imaging system (Bio-Rad Laboratories, Inc.).

Secretome treatment. Secretome was collected from shHSPD1-A549 and shControl-A549 cells according to the protocol described in the previous study (19). Briefly, an equal number of shHSPD1-A549 and shControl-A549 cells

were seeded in complete medium overnight. After washing with PBS, the cells were incubated in serum-free DMEM for 24 h. The collected supernatants were centrifuged at 1,000 x g for 5 min at 4˚C to remove debris and used for subsequent experiments. Cell proliferation, total cell number and VEGF levels in the secretome of shHSPD1-A549 and shControl-A549 cells were assessed. Total cell number of shHSPD1-A549 and shControl-A549 cells after incubation in serum-free DMEM for 24 h was determined by trypan blue staining. The cells were harvested, resuspended in PBS, and stained with 0.4% trypan blue solution (Gibco, Thermo Fisher Scientific, USA) at a 1:1 ratio for 2 min at room temperature. The stained cell suspension was loaded onto a hemocytometer. Total cell number was counted under a Zeiss Primovert inverted microscope (Zeiss GmbH).

For EA.hy926 cell treatment, secretome, derived from an equal number of cells was mixed with serum-free DMEM at a 1:1 (v/v) ratio. EA.hy926 cells were initially plated in complete medium and incubated at 37˚C overnight. After washing with PBS, the cells were treated with either shControl or shHSPD1 secretome at 37˚C for 24 h. Cells incubated with serum-free DMEM served as untreated controls. The morphology of EA.hy926 cells was observed and captured using a Zeiss Primovert inverted microscope (Zeiss GmbH).

MTT assay. Cell viability was evaluated using the MTT assay. Following 24 h of secretome treatment, EA.hy926 cells were exposed to 0.5 mg/ml MTT solution. After incubation, the solution was discarded and dimethyl sulfoxide was added to dissolve the resulting formazan crystals. Absorbance was recorded at 570 nm using a Tecan Spark multimode microplate reader (Tecan Group, Ltd.). Cell viability was expressed as a percentage relative to the untreated control group.

BrdU assay. Cell proliferation was determined using a BrdU Cell Proliferation ELISA Kit (ab126556; Abcam) according to the manufacturer's instructions. EA.hy926 cells were seeded in a 96-well plate and treated with the secretome for 24 h. After incubation with BrdU solution for 2 h, the cells were fixed using a fixing solution (included in the kit) for 30 min at room temperature. The fixed cells were then incubated with a primary anti-BrdU antibody, followed by a horseradish peroxidase-conjugated secondary antibody. Subsequently, 3,3',5,5'-tetramethylbenzidine substrate was added and the absorbance at 450 nm was measured using a Tecan Spark multimode microplate reader (Tecan Group, Ltd.). Cell proliferation was calculated as a fold change relative to the untreated control group.

Wound healing-scratch assay. Cell migration was assessed using a wound healing-scratch assay, as previously described (19). A 200-μl pipette tip was used to scratch the EA.hy926 cell monolayers and detached cells were removed by washing with PBS. The remaining cells were treated with secretome, without FBS supplementation, and images of the scratch area were captured at various time points (0, 8, 16 and 24 h after treatment with secretome) using an IX83 inverted microscope (Olympus Corporation) equipped with an STX stage-top incubator (Tokai Hit). Image analysis was performed using ImageJ version 1.54d (National Institutes of Health) with the wound healing size tool plugin (25). The percentage of wound healing was calculated using the formula: Percentage of wound healing=100% x (initial wound size - wound size at each time point)/initial wound size.

Cell invasion assay. Cell invasion was determined using Transwell invasion assay. Transwell inserts with an 8 μm pore size (Corning Inc., Corning, NY, USA) were pre-coated with Matrigel Basement Membrane Matrix (Corning Inc.) at 37˚C overnight, following the manufacturer's instructions. EA.hy926 cells were seeded into the upper chamber of each insert in a serum-free medium containing either shControl or shHSPD1 secretome, while the lower chamber was filled with DMEM supplemented with 20% FBS. After a 24-h incubation, cells remaining on the upper surface of the membrane were removed with a cotton swab. The filters were washed with PBS, fixed with 4% formaldehyde in PBS for 10 min and stained with 0.5% crystal violet for 20 min. Images of stained cells were captured using a Zeiss Primovert inverted microscope (Zeiss GmbH). Crystal violet bound to the cells was then dissolved in 33% acetic acid and absorbance was measured at 590 nm using a Tecan Spark multimode microplate reader (Tecan Group, Ltd.). Cell invasion was expressed as a fold change relative to the untreated control group.

Cell aggregation assay. Cell aggregation was assessed using a hanging drop assay, as previously described (26). EA.hy926 cells were detached from the monolayer culture using trypsinization and then resuspended in a serum-free medium containing either shControl or shHSPD1 secretome at a concentration of 5,000 cells/ml. Drops of 20 μl of the cell suspension were placed on the inner side of the lid of a 100-mm tissue culture dish. To maintain humidity, 5 ml of PBS was added to the bottom of the dish and the lid was inverted to cover it. After 24-h incubation, a total of 30 drops per group were collected, dispersed by gentle pipetting and examined for multicellular spheroid formation using a Zeiss Primovert inverted microscope (Zeiss GmbH). The sizes of spheroids were measured from 30 cell aggregates for each sample using ImageJ version 1.54d (National Institutes of Health) (27).

Endothelial tube formation assay. Capillary-like tube formation by EA.hy926 cells was assessed on 96-well plates pre-coated with Matrigel® Basement Membrane Matrix (Corning Inc.). Each well was coated with 50 μl of Matrigel and incubated at 37˚C for 30 min to allow for solidification. Following a 24-h treatment with either shControl or shHSPD1 secretome, EA.hy926 cells were detached and seeded onto the solidified Matrigel at a density of $5x10^4$ cells per well. The cells were then incubated in DMEM supplemented with 10% FBS for an additional 24 h. Tube formation was visualized using an IX83 inverted microscope (Olympus) with an STX stage-top incubator (Tokai Hit). Tube length and area were quantified from 30 tube formations for each sample using ImageJ version 1.54d (National Institutes of Health) (27).

ELISA. The concentration of VEGF in the culture supernatant of EA.hy926 cells following secretome treatment was measured using a human VEGF ELISA Kit (cat. no. ab222510; Abcam), following the manufacturer's protocol. VEGF levels were determined from a standard curve.

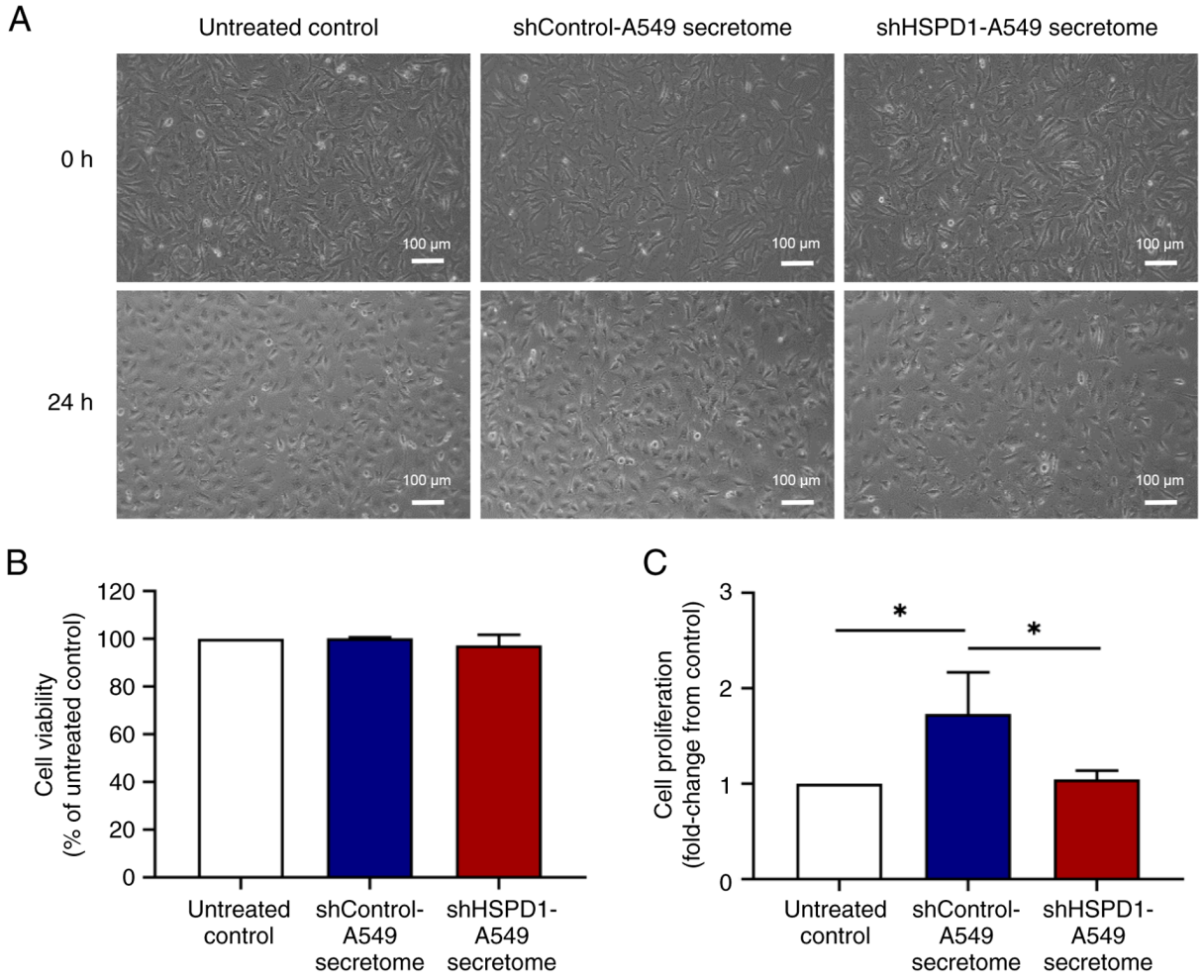

Figure 1. Morphology, viability and proliferation of EA.hy926 cells after treatment with shHSPD1-A549 and shControl-A549 secretomes. (A) Morphology of EA.hy926 cells observed under an inverted microscope, captured at x100 magnification. (B) Viability of EA.hy926 cells after 24-h treatment with secretomes, determined by MTT assay. Data are presented as a percentage of the untreated control. (C) Proliferation of EA.hy926 cells measured using the BrdU assay after 24-h treatment with secretomes. Data are shown as a fold change relative to the untreated control. Bar graphs represent mean ± SD from three independent experiments. *P<0.05. sh, short hairpin.

Bioinformatic analysis. The correlation between VEGFA and HSPD1 mRNA expression was analyzed in The Cancer Genome Atlas-Lung Adenocarcinoma (TCGA-LUAD) cohort (n=515) using the Tumor IMmune Estimation Resource (TIMER) database (https://cistrome.shinyapps.io/timer/) (28,29). Spearman's ϱ and P-values were calculated by the database. The association between VEGFA mRNA expression and overall survival in patients with lung adenocarcinoma was evaluated in a lung adenocarcinoma cohort (n=1,863) using the Kaplan-Meier Plotter database (https://www.kmplot.com) (30). Patients were divided into low- and high-expression groups based on the median VEGFA mRNA expression levels (Affymetrix ID: 210513_s_at). The hazard ratio and log-rank P-value were computed by the database.

Statistical analysis. Quantitative data are presented as mean ± SD. Comparisons between two groups were conducted using an unpaired t-test, while multiple group comparisons were performed using one-way analysis of variance (ANOVA) followed by Tukey's post-hoc test. Statistical analyses were conducted using GraphPad Prism version 8.0.1 (Dotmatics). P<0.05 was considered to indicate a statistically significant difference.

Results

Effect of shHSPD1-A549 and shControl-A549 secretomes on EA.hy926 cell proliferation. The secretome was derived from an equal number of shHSPD1-A549 and shControl-A549 cells. At the time of secretome collection, no significant difference in cell proliferation and total cell number was observed (Fig. S1). Additionally, VEGF levels in the shHSPD1-A549 and shControl-A549 secretomes showed no significant difference (Fig. S1). These secretomes were then used to treat EA.hy926 cells. After 24-h of treatment, the cell morphology of EA.hy926 cells was observed under an inverted microscope. As shown in Fig. 1A, no morphological signs of cytotoxicity were observed following treatment with either the shHSPD1-A549 or shControl-A549 secretomes. Results of MTT assay further confirmed that these secretomes had no significant cytotoxic effect on EA.hy926 cells (Fig. 1B). Notably, the results of BrdU assay demonstrated that the shControl-A549 secretome markedly promoted cell proliferation, while the shHSPD1-A549

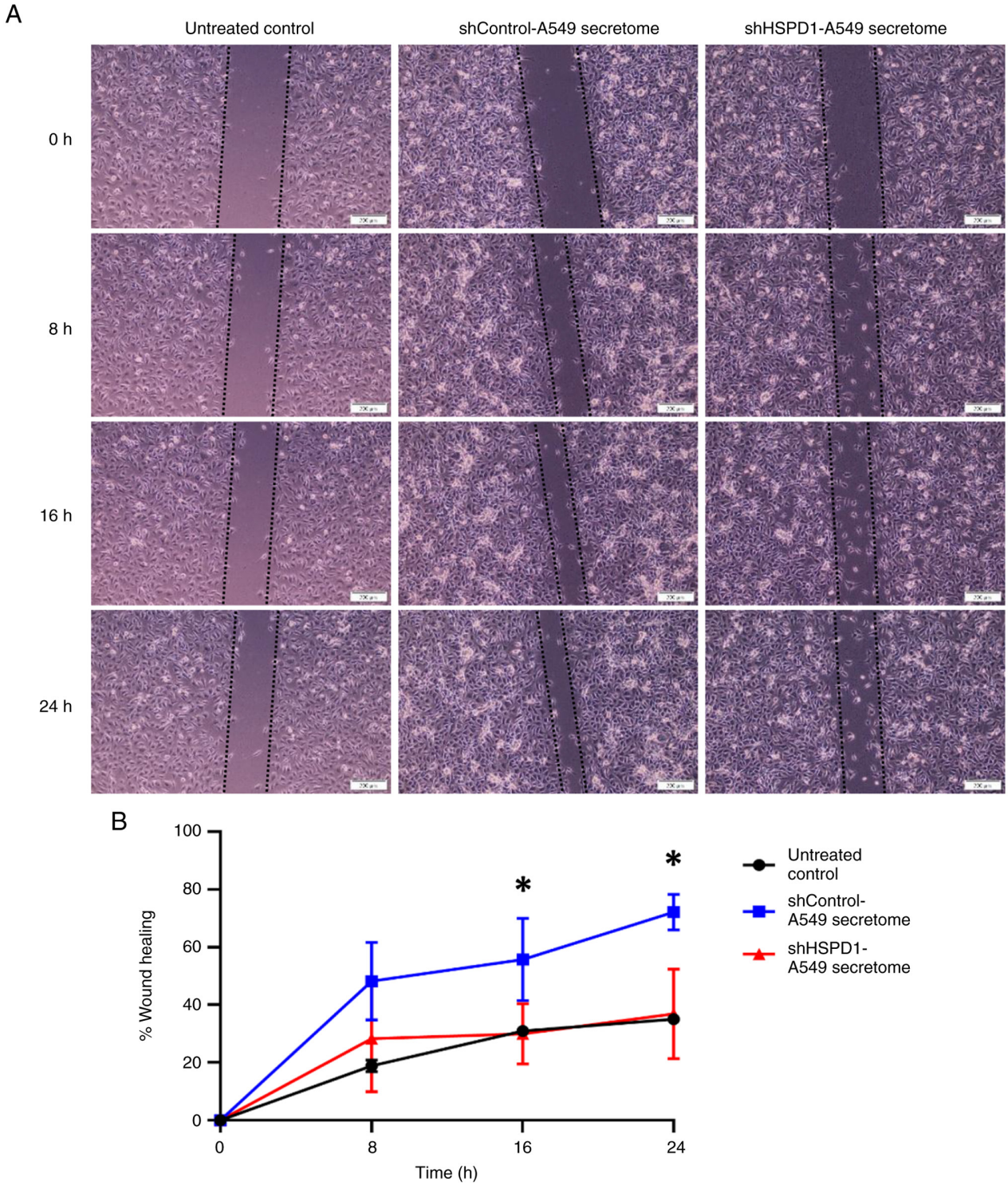

Figure 2. Cell migration capability of EA.hy926 cells after treatment with shHSPD1-A549 and shControl-A549 secretomes. (A) Representative images of the wound area captured at 0, 8, 16 and 24 h after secretome treatment, captured at x100 magnification. (B) Percentage of wound healing. Data are presented as mean ± SD from three independent experiments. *P<0.05. sh, short hairpin; HSPD1, heat shock protein family D member 1.

secretome showed no stimulatory effect (Fig. 1C). These findings suggested that HSPD1 might play a role in stimulating endothelial cell proliferation.

Effect of shHSPD1-A549 and shControl-A549 secretomes on EA.hy926 cell migration. The effect of shHSPD1-A549 and shControl-A549 secretomes on EA.hy926 cell migration was evaluated using a wound healing-scratch assay. Results indicated that the percentage of wound healing increased gradually with extended incubation time. Cells treated with the shControl-A549 secretome showed a markedly higher percentage of wound healing at the 16- and 24-h time points. By contrast, no significant difference was observed between cells treated with the shHSPD1-A549 secretome and the untreated control group (Fig. 2). These findings suggested that HSPD1 could enhance migration capability of endothelial cells.

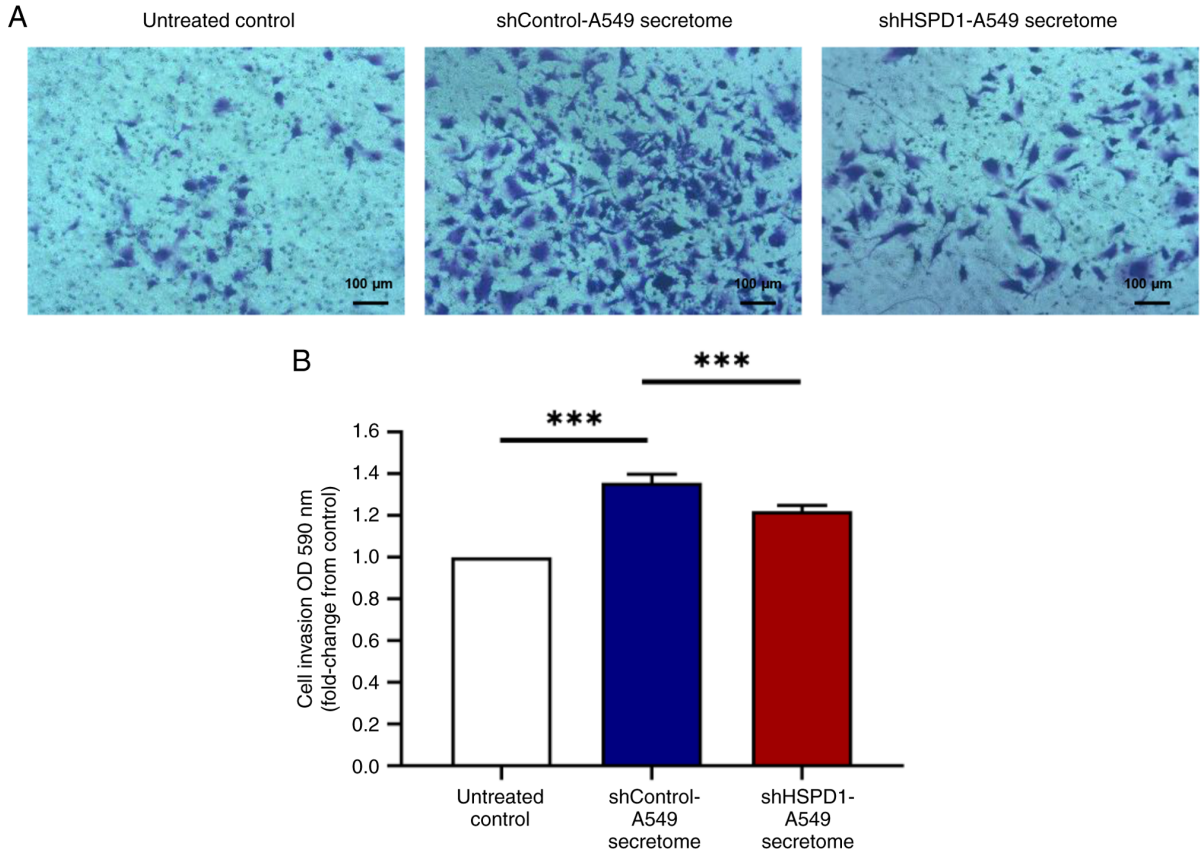

Figure 3. Cell invasion of EA.hy926 cells after treatment with shHSPD1-A549 and shControl-A549 secretomes. (A) Representative images of crystal violet-stained EA.hy926 cells after 24-h treatment with secretomes, captured at x100 magnification. (B) The optical density of crystal violet-stained cells at 590 nm. Data are presented as mean ± SD from three independent experiments and expressed as a fold change relative to the untreated control. ***P<0.001. sh, short hairpin; HSPD1, heat shock protein family D member 1.

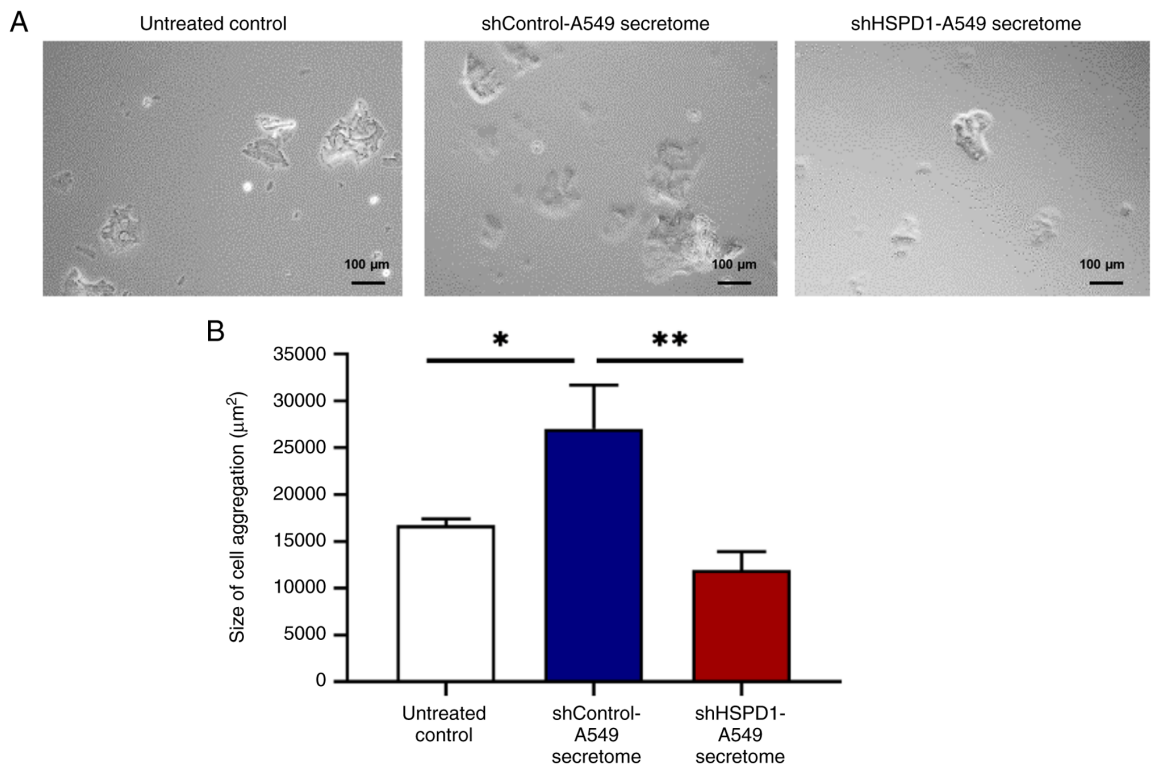

Figure 4. Cell aggregation of EA.hy926 cells following treatment with shHSPD1-A549 and shControl-A549 secretomes. (A) Representative images of EA.hy926 cell aggregates after secretome treatment, captured at x100 magnification. (B) Size of cell aggregates. Data are presented as mean ± SD from three independent experiments. *P<0.05, **P<0.01. sh, short hairpin; HSPD1, heat shock protein family D member 1.

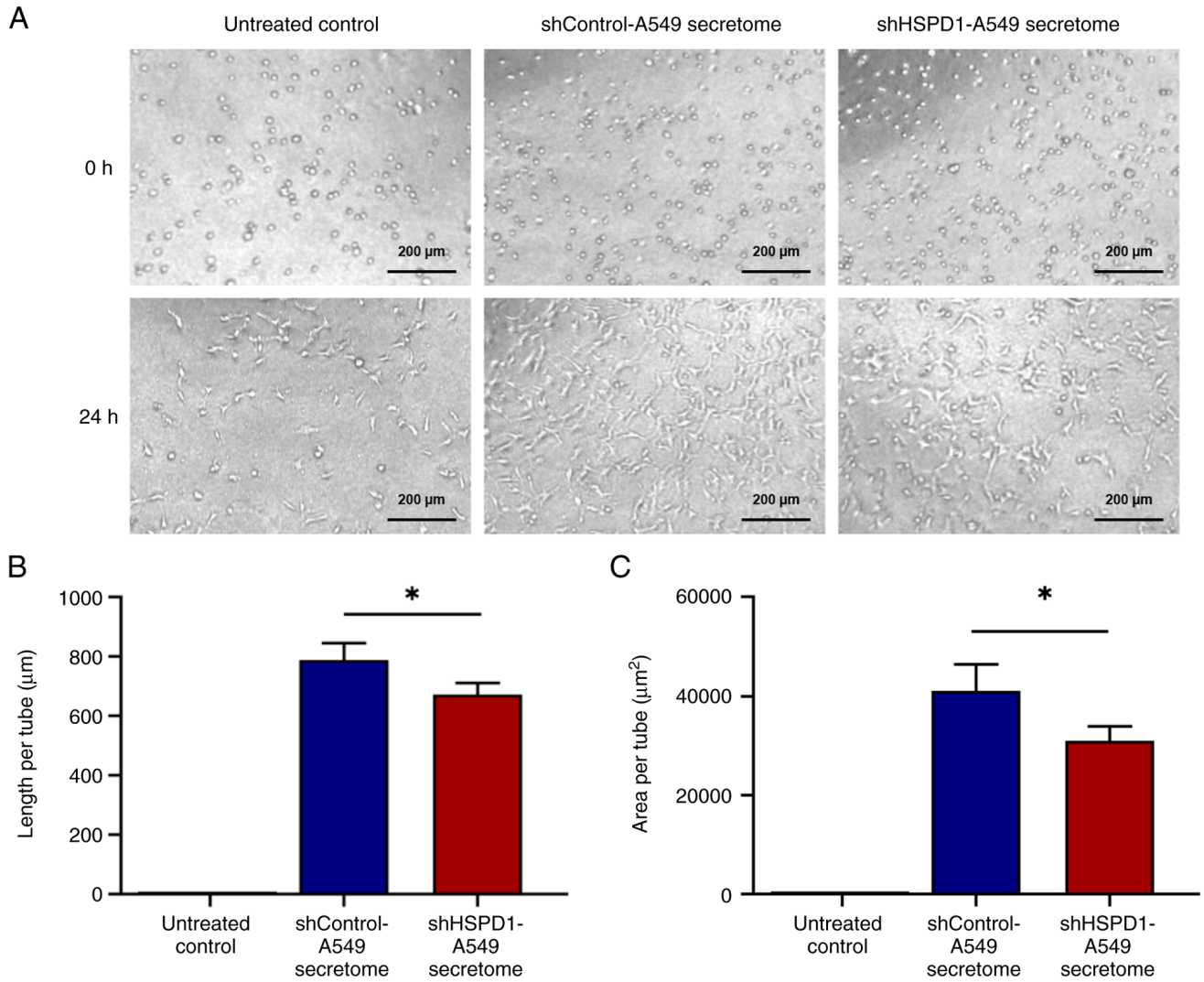

Figure 5. Endothelial tube formation of EA.hy926 cells after treatment with shHSPD1-A549 and shControl-A549 secretomes. (A) Representative images of tube formation in EA.hy926 cells after secretome treatment, captured at x40 magnification with additional zoomed-in areas. (B) Length of formed tubes. (C) Area of formed tubes. Data are presented as mean ± SD from three independent experiments. *P<0.05. sh, short hairpin; HSPD1, heat shock protein family D member 1.

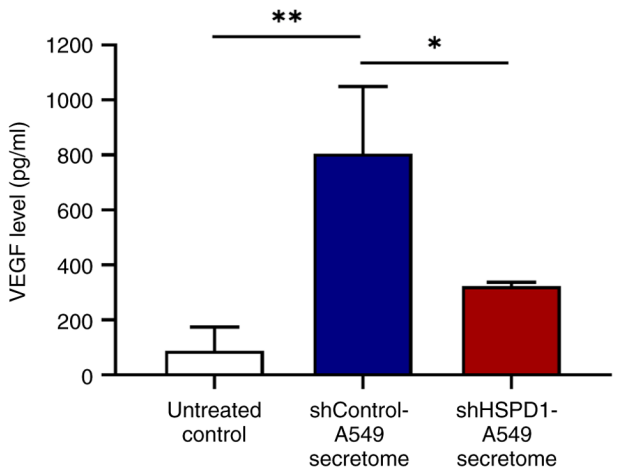

Figure 6. VEGF levels in the culture supernatant of EA.hy926 cells after treatment with shHSPD1-A549 and shControl-A549 secretomes. VEGF levels were measured by ELISA. The bar graph represents mean ± SD from three independent experiments. *P<0.05, **P<0.01. VEGF, vascular endothelial growth factor; sh, short hairpin; HSPD1, heat shock protein family D member 1.

Effect of shHSPD1-A549 and shControl-A549 secretomes on EA.hy926 cell invasiveness. A Transwell invasion assay was performed to assess the invasiveness of EA.hy926 cells following secretome treatment. The shControl-A549 secretome markedly enhanced invasion of EA.hy926 cells, while the secretome from HSPD1 knockdown did not increase cell invasion (Fig. 3). These findings indicated a crucial role of HSPD1 in promoting invasion of endothelial cells.

Effect of shHSPD1-A549 and shControl-A549 secretomes on EA.hy926 cell aggregation. A hanging-drop assay was performed to assess the effect of shHSPD1-A549 and shControl-A549 secretomes on cell aggregation in EA.hy926 cells. As shown in Fig. 4, the shControl-A549 secretome promoted cell aggregation in EA.hy926 cells. The size of cell aggregates appeared similar between cells treated with the shHSPD1-A549 secretome and those in the untreated control group, indicating that HSPD1 may contribute to lung cancer-induced cell aggregation in EA.hy926 cells.

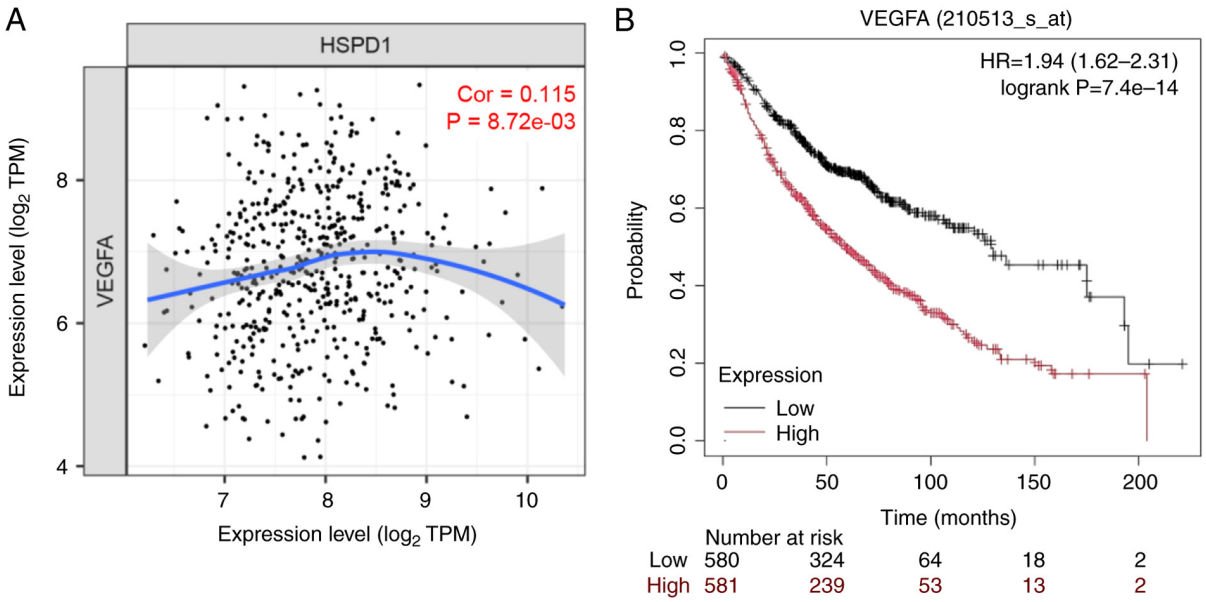

Figure 7. Correlation of VEGFA expression with HSPD1 expression and overall survival in patients with lung adenocarcinoma. (A) Scatter plot showing the correlation between VEGFA and HSPD1 expression in the TCGA-LUAD cohort, analyzed using the TIMER database. (B) Kaplan-Meier survival curve comparing overall survival in lung adenocarcinoma patients with low and high VEGFA expression, obtained from the KM Plotter database. VEGF, vascular endothelial growth factor; sh, short hairpin; HSPD1, heat shock protein family D member 1; TCGA-LUAD, The Cancer Genome Atlas-Lung Adenocarcinoma; TIMER, Tumor IMmune Estimation Resource.

Effect of shHSPD1-A549 and shControl-A549 secretomes on endothelial tube formation in EA.hy926 cells. To assess the angiogenic potential of EA.hy926 cells in response to secretome treatment, a tube formation assay was conducted. No tube formation was observed in the untreated control group. By contrast, EA.hy926 cells treated with the shControl-A549 secretome could form a network of tubular structure, which was markedly longer and larger than the tubular structure of EA.hy926 cells treated with the shHSPD1-A549 secretome (Fig. 5). These findings suggested that HSPD1 may play a critical role in tube formation of EA.hy926 cells.

Effect of shHSPD1-A549 and shControl-A549 secretomes on VEGF secretion from EA.hy926 cells. Given the role of VEGF as a key pro-angiogenic factor in cancer-induced angiogenesis (8), VEGF levels in the culture supernatant of EA.hy926 cells treated with shHSPD1-A549 and shControl-A549 secretomes were measured by ELISA. Consistent with its stimulatory effect on tube formation, the shControl-A549 secretome markedly increased VEGF secretion. By contrast, cells treated with the shHSPD1-A549 secretome exhibited lower VEGF levels, suggesting that HSPD1 may induce VEGF-mediated angiogenesis in lung cancer (Fig. 6).

Correlation of VEGFA expression with HSPD1 expression and overall survival in patients with lung adenocarcinoma. The TIMER database was used to assess the correlation between VEGFA and HSPD1 expression in the TCGA-LUAD cohort. The results showed that VEGFA expression was markedly associated with HSPD1 expression in lung adenocarcinoma (Fig. 7A). Additionally, the relationship between VEGFA expression and overall survival in lung adenocarcinoma patients was evaluated. Data from the KM Plotter database revealed that patients with high VEGFA expression had poorer survival outcomes compared to those with low VEGFA expression (Fig. 7B). These findings highlighted the clinical relevance of HSPD1 and VEGFA, as well as the prognostic significance of VEGFA in lung cancer patients.

Discussion

Angiogenesis is recognized as a hallmark of cancer that plays a pivotal role in tumor growth and metastasis (7). HSPD1 has been implicated in various cancers due to its roles in regulating apoptosis, metabolism and immune responses (14,15). It has been shown to regulate endothelial cell function and the secretion of pro-angiogenic factors, such as VEGF (20-24). Previous studies have demonstrated that HSPD1 not only exerts its oncogenic effects on lung cancer cells (17), but also modulates the TME to further support cancer growth and progression (18,19). Knockdown of HSPD1 in lung cancer cells has been shown to alter secretory protein composition and reduce their activity in activating CAFs (19). Notably, the secretome from shHSPD1-knockdown cells exhibited decreased levels of HSPD1 (19). These findings suggested that HSPD1 may also play a role in regulating other cells within the TME, including endothelial cells.

As secreted proteins are present in very limited amounts in the culture medium, concentration and preparation steps are required for accurate quantification (31). To minimize variations and ensure consistency, the secretome in the present study was collected from an equal number of shHSPD1-A549 and shControl-A549 cells. There was no significant difference in cell proliferation and cell number at the time of secretome collection. Therefore, it was considered that biomolecules were present in comparable amounts in the secretomes of these two cell groups. Additionally, VEGF levels in the shHSPD1-A549 and shControl-A549 secretomes showed no significant

difference, suggesting that other secreted proteins may play key roles in regulating angiogenesis in lung cancer.

Previous studies have demonstrated that secreted proteins from lung cancer cells promote endothelial cell proliferation, migration and angiogenesis (32-34). Consistent with these findings, the present study revealed that treatment with the secretome from shControl-A549 cells markedly enhanced endothelial cell proliferation, migration, invasion, aggregation and tube formation. By contrast, the secretome from shHSPD1-A549 cells showed no significant effects on these processes. These results suggested that HSPD1 may serve as a key regulator of endothelial cell behavior and angiogenesis. However, the wound healing-scratch and Transwell invasion assays used in the present study could not distinguish the effects of cell proliferation from those of migration and invasion (35). Additional experiments using proliferation inhibitors are needed to more precisely define the role of the secretome in endothelial cell migration and invasion.

The mechanism by which HSPD1 promotes angiogenesis is not fully understood. However, the findings of the present study suggested that HSPD1 may induce VEGF-mediated angiogenesis. VEGF is a potent pro-angiogenic factor that stimulates endothelial cell proliferation, migration and tube formation (8). A recent study demonstrates that HSPD1 enhances the protein stability and secretion of VEGF in colorectal cancer (24). Additionally, HSPD1 is recognized as a ligand for Toll-like receptor 4 (TLR4) (36,37), whose signaling plays a critical role in regulating endothelial cell functions (38). Activation of TLR4 promotes the secretion of cytokines and pro-angiogenic factors, including VEGF (39,40). Therefore, HSPD1 may induce VEGF secretion through mechanisms involving TLR4 and its downstream signaling pathways, contributing to angiogenesis in lung cancer. However, further experiments using recombinant HSPD1 protein are needed to clarify its role in angiogenesis and the underlying mechanisms.

VEGF exerts its effects by binding to its receptors, VEGFRs, leading to the activation of various downstream signaling pathways, such as phospholipase C, phosphoinositide 3-kinase/protein kinase B and mitogen-activated protein kinase kinase/extracellular signal-regulated kinase signaling pathways, which are critical for promoting angiogenesis (8,12). In addition to regulating endothelial cell functions, VEGF modulates the anti-tumor immune response within the tumor microenvironment (8,12). VEGF can promote an immunosuppressive environment by inhibiting the activity of immune cells such as cytotoxic T cells and dendritic cells (41,42). These findings suggest that HSPD1 may promote angiogenesis and contribute to an immunosuppressive environment in lung cancer by enhancing VEGF secretion from endothelial cells.

In addition, HSPD1 knockdown in lung cancer cells leads to a significant decrease in other secretory proteins, including HSP90 and prohibitin-1 (PHB1) (19), both of which are implicated in angiogenesis (43,44). Secreted HSP90 has been shown to promote endothelial cell migration and tube formation (43), while PHB1 regulates angiogenesis by modulating mitochondrial functions (44). These observations suggest that HSPD1 may influence angiogenesis not only directly but also through the regulation of other pro-angiogenic secreted proteins. Further studies are required to explore the interplay between HSPD1 and these proteins in lung cancer-induced angiogenesis.

The present study has several limitations that should be addressed. First, the precise molecular mechanisms by which HSPD1 modulates endothelial cell behavior remain unclear. Second, the use of *in vitro* models with EA.hy926 cells and lung cancer cell secretomes may not fully recapitulate the complexity of the TME *in vivo*. Third, the contributions of other secretory proteins, such as HSP90 and PHB1, to angiogenesis in lung cancer were not independently validated. Additionally, the immunosuppressive role of VEGF in the TME was not explored. Finally, the present study did not include experiments using recombinant HSPD1 protein to directly evaluate its effects on endothelial cell behavior and underlying mechanisms. Future research addressing these limitations will provide a deeper understanding of the role of HSPD1 in lung cancer-induced angiogenesis and its potential as a therapeutic target.

In conclusion, the present study demonstrated the role of HSPD1 in promoting cell proliferation, migration, invasion, aggregation and angiogenesis in endothelial cells, potentially through VEGF-mediated pathways. Targeting HSPD1 may be a promising therapeutic strategy for inhibiting tumor angiogenesis and preventing tumor progression.

Acknowledgments

Not applicable.

Funding

The present study was supported by the Thailand Science Research and Innovation (TSRI) (grant no. 672A07023) and the TSRI, Chulabhorn Research Institute (grant no. 49890/4759797).

Availability of data and materials

The data generated in the present study may be requested from the corresponding author.

Authors' contributions

KS and SA contributed to the conception and design of the study, performed experiments, analyzed data, created visualizations and were major contributors to manuscript writing. KS also managed the project and secured funding. AR, ATM, PH and JN conducted experiments. ANM and SK contributed to data analysis and supplied resources. KL, SP and JS contributed to data analysis and supervised the project. KS and SA confirm the authenticity of all raw data. All authors read and approved the final manuscript.

Ethics approval and consent to participate

Not applicable.

Patient consent for publication

Not applicable.

Competing interest

The authors declare that they have no competing interests.

References

1. Folkman J: Role of angiogenesis in tumor growth and metastasis. Semin Oncol 29 (6 Suppl 16): S15-S18, 2002.
2. Li Y, Lin M, Wang S, Cao B, Li C and Li G: Novel angiogenic regulators and anti-angiogenesis drugs targeting angiogenesis signaling pathways: Perspectives for targeting angiogenesis in lung cancer. Front Oncol 12: 842960, 2022.
3. Altorki NK, Markowitz GJ, Gao D, Port JL, Saxena A, Stiles B, McGraw T and Mittal V: The lung microenvironment: an important regulator of tumour growth and metastasis. Nat Rev Cancer 19: 9-31, 2019.
4. Hwang I, Kim JW, Ylaya K, Chung EJ, Kitano H, Perry C, Hanaoka J, Fukuoka J, Chung JY and Hewitt SM: Tumor-associated macrophage, angiogenesis and lymphangiogenesis markers predict prognosis of non-small cell lung cancer patients. J Transl Med 18: 443, 2020.
5. Bremnes RM, Camps C and Sirera R: Angiogenesis in non-small cell lung cancer: The prognostic impact of neoangiogenesis and the cytokines VEGF and bFGF in tumours and blood. Lung Cancer 51: 143-158, 2006.
6. Gu X, Chu L and Kang Y: Angiogenic factor-based signature predicts prognosis and immunotherapy response in non-small-cell lung cancer. Front Genet 13: 894024, 2022.
7. Majidpoor J and Mortezaee K: Angiogenesis as a hallmark of solid tumors-clinical perspectives. Cell Oncol (Dordr) 44: 715-737, 2021.
8. Ghalehbandi S, Yuzugulen J, Pranjol MZI and Pourgholami MH: The role of VEGF in cancer-induced angiogenesis and research progress of drugs targeting VEGF. Eur J Pharmacol 949: 175586, 2023.
9. Lee S, Chen TT, Barber CL, Jordan MC, Murdock J, Desai S, Ferrara N, Nagy A, Roos KP and Iruela-Arispe ML: Autocrine VEGF signaling is required for vascular homeostasis. Cell 130: 691-703, 2007.
10. Liu Y, Cox SR, Morita T and Kourembanas S: Hypoxia regulates vascular endothelial growth factor gene expression in endothelial cells. Identification of a 5' enhancer. Circ Res 77: 638-643, 1995.
11. Du H, Shi H, Chen D, Zhou Y and Che G: Cross-talk between endothelial and tumor cells via basic fibroblast growth factor and vascular endothelial growth factor signaling promotes lung cancer growth and angiogenesis. Oncol Lett 9: 1089-1094, 2015.
12. Zhao Y, Guo S, Deng J, Shen J, Du F, Wu X, Chen Y, Li M, Chen M, Li X, *et al*: VEGF/VEGFR-targeted therapy and immunotherapy in non-small cell lung cancer: Targeting the tumor microenvironment. Int J Biol Sci 18: 3845-3858, 2022.
13. Vakhrushev IV, Nezhurina EK, Karalkin PA, Tsvetkova AV, Sergeeva NS, Majouga AG and Yarygin KN: Heterotypic multicellular spheroids as experimental and preclinical models of sprouting angiogenesis. Biology (Basel) 11: 18, 2021.
14. Yun CW, Kim HJ, Lim JH and Lee SH: Heat shock proteins: Agents of cancer development and therapeutic targets in anti-cancer therapy. Cells 9: 60, 2019.
15. Quintana FJ and Cohen IR: The HSP60 immune system network. Trends Immunol 32: 89-95, 2011.
16. Tang Y, Yang Y, Luo J, Liu S, Zhan Y, Zang H, Zheng H, Zhang Y, Feng J, Fan S and Wen Q: Overexpression of HSP10 correlates with HSP60 and Mcl-1 levels and predicts poor prognosis in non-small cell lung cancer patients. Cancer Biomark 30: 85-94, 2021.
17. Parma B, Ramesh V, Gollavilli PN, Siddiqui A, Pinna L, Schwab A, Marschall S, Zhang S, Pilarsky C, Napoli F, *et al*: Metabolic impairment of non-small cell lung cancers by mitochondrial HSPD1 targeting. J Exp Clin Cancer Res 40: 248, 2021.
18. Aluksanasuwan S, Somsuan K, Ngoenkam J, Chutipongtanate S and Pongcharoen S: Potential association of HSPD1 with dysregulations in ribosome biogenesis and immune cell infiltration in lung adenocarcinoma: An integrated bioinformatic approach. Cancer Biomark 39: 155-170, 2024.
19. Aluksanasuwan S, Somsuan K, Ngoenkam J, Chiangjong W, Rongjumnong A, Morchang A, Chutipongtanate S and Pongcharoen S: Knockdown of heat shock protein family D member 1 (HSPD1) in lung cancer cell altered secretome profile and cancer-associated fibroblast induction. Biochim Biophys Acta Mol Cell Res 187: 119736, 2024.
20. Duan Y, Tang H, Mitchell-Silbaugh K, Fang X, Han Z and Ouyang K: Heat shock protein 60 in cardiovascular physiology and diseases. Front Mol Biosci 7: 73, 2020.
21. Qiu J, Gao HQ, Liang Y, Yu H and Zhou RH: Comparative proteomics analysis reveals role of heat shock protein 60 in digoxin-induced toxicity in human endothelial cells. Biochim Biophys Acta 1784: 1857-1864, 2008.
22. Billack B, Heck DE, Mariano TM, Gardner CR, Sur R, Laskin DL and Laskin JD: Induction of cyclooxygenase-2 by heat shock protein 60 in macrophages and endothelial cells. Am J Physiol Cell Physiol 283: C1267-C1277, 2002.
23. Lin CS, He PJ, Hsu WT, Wu MS, Wu CJ, Shen HW, Hwang CH, Lai YK, Tsai NM and Liao KW: Helicobacter pylori-derived heat shock protein 60 enhances angiogenesis via a CXCR2-mediated signaling pathway. Biochem Biophys Res Commun 397: 283-289, 2010.
24. Zheng D, Zhang X, Xu J, Chen S, Wang B and Yuan X: LncRNA LINC01503 promotes angiogenesis in colorectal cancer by regulating VEGFA expression via miR-342-3p and HSP60 binding. J Biomed Res: Oct 25, 2024 (Epub ahead of print).
25. Suarez-Arnedo A, Torres Figueroa F, Clavijo C, Arbeláez P, Cruz JC and Muñoz-Camargo C: An image J plugin for the high throughput image analysis of in vitro scratch wound healing assays. PLoS One 15: e0232565, 2020.
26. Somsuan K, Peerapen P, Boonmark W, Plumworasawat S, Samol R, Sakulsak N and Thongboonkerd V: ARID1A knockdown triggers epithelial-mesenchymal transition and carcinogenesis features of renal cells: Role in renal cell carcinoma. FASEB J 33: 12226-12239, 2019.
27. Schneider CA, Rasband WS and Eliceiri KW: NIH Image to ImageJ: 25 years of image analysis. Nat Methods 9: 671-675, 2012.
28. Li T, Fan J, Wang B, Traugh N, Chen Q, Liu JS, Li B and Liu XS: TIMER: A web server for comprehensive analysis of tumor-infiltrating immune cells. Cancer Res 77: e108-e110, 2017.
29. Li B, Severson E, Pignon JC, Zhao H, Li T, Novak J, Jiang P, Shen H, Aster JC, Rodig S, *et al*: Comprehensive analyses of tumor immunity: Implications for cancer immunotherapy. Genome Biol 17: 174, 2016.
30. Győrffy B: Transcriptome-level discovery of survival-associated biomarkers and therapy targets in non-small-cell lung cancer. Br J Pharmacol 181: 362-374, 2024.
31. Makridakis M and Vlahou A: Secretome proteomics for discovery of cancer biomarkers. J Proteomics 73: 2291-2305, 2010.
32. da Cunha BR, Domingos C, Stefanini ACB, Henrique T, Polachini GM, Castelo-Branco P and Tajara EH: Cellular interactions in the tumor microenvironment: The role of secretome. J Cancer 10: 4574-4587, 2019.
33. Cheng HW, Chen YF, Wong JM, Weng CW, Chen HY, Yu SL, Chen HW, Yuan A and Chen JJ: Cancer cells increase endothelial cell tube formation and survival by activating the PI3K/Akt signalling pathway. J Exp Clin Cancer Res 36: 27, 2017.
34. Zhong L, Roybal J, Chaerkady R, Zhang W, Choi K, Alvarez CA, Tran H, Creighton CJ, Yan S, Strieter RM, *et al*: Identification of secreted proteins that mediate cell-cell interactions in an in vitro model of the lung cancer microenvironment. Cancer Res 68: 7237-7245, 2008.
35. Kramer N, Walzl A, Unger C, Rosner M, Krupitza G, Hengstschläger M and Dolznig H: In vitro cell migration and invasion assays. Mutat Res 752: 10-24, 2013.
36. Tian J, Guo X, Liu XM, Liu L, Weng QF, Dong SJ, Knowlton AA, Yuan WJ and Lin L: Extracellular HSP60 induces inflammation through activating and up-regulating TLRs in cardiomyocytes. Cardiovasc Res 98: 391-401, 2013.
37. Vabulas RM, Ahmad-Nejad P, da Costa C, Miethke T, Kirschning CJ, Häcker H and Wagner H: Endocytosed HSP60s use toll-like receptor 2 (TLR2) and TLR4 to activate the toll/interleukin-1 receptor signaling pathway in innate immune cells. J Biol Chem 276: 31332-31339, 2001.
38. Stierschneider A and Wiesner C: Shedding light on the molecular and regulatory mechanisms of TLR4 signaling in endothelial cells under physiological and inflamed conditions. Front Immunol 14: 1264889, 2023.
39. Pei Z, Lin D, Song X, Li H and Yao H: TLR4 signaling promotes the expression of VEGF and TGFbeta1 in human prostate epithelial PC3 cells induced by lipopolysaccharide. Cell Immunol 254: 20-27, 2008.

40. Riddell JR, Maier P, Sass SN, Moser MT, Foster BA and Gollnick SO: Peroxiredoxin 1 stimulates endothelial cell expression of VEGF via TLR4 dependent activation of HIF-1α. PLoS One 7: e50394, 2012.
41. Voron T, Colussi O, Marcheteau E, Pernot S, Nizard M, Pointet AL, Latreche S, Bergaya S, Benhamouda N, Tanchot C, *et al*: VEGF-A modulates expression of inhibitory checkpoints on CD8+ T cells in tumors. J Exp Med 212: 139-148, 2015.
42. Gabrilovich D, Ishida T, Oyama T, Ran S, Kravtsov V, Nadaf S and Carbone DP: Vascular endothelial growth factor inhibits the development of dendritic cells and dramatically affects the differentiation of multiple hematopoietic lineages in vivo. Blood 92: 4150-4166, 1998.
43. Song X and Luo Y: The regulatory mechanism of Hsp90alpha secretion from endothelial cells and its role in angiogenesis during wound healing. Biochem Biophys Res Commun 398: 111-117, 2010.
44. Schleicher M, Shepherd BR, Suarez Y, Fernandez-Hernando C, Yu J, Pan Y, Acevedo LM, Shadel GS and Sessa WC: Prohibitin-1 maintains the angiogenic capacity of endothelial cells by regulating mitochondrial function and senescence. J Cell Biol 180: 101-112, 2008.